

Topology and the suppression of CMB large-angle correlations

Armando Bernui,^{1,*} Camila P. Novaes,^{1,†} Thiago S. Pereira,^{2,‡} and Glenn D. Starkman^{3,§}

¹*Observatório Nacional, Rua General José Cristino 77,
São Cristóvão, 20921-400 Rio de Janeiro – RJ, Brazil*

²*Departamento de Física, Universidade Estadual de Londrina,*

Rodovia Celso Garcia Cid, km 380, 86051-990, Londrina – PR, Brazil

³*CERCA/ISO/Physics Department, Case Western Reserve University, Cleveland, OH 44106-7079, USA*

(Dated: November 25, 2021)

To date, no compelling evidence has been found that the universe has non-trivial spatial topology. Meanwhile, anomalies in the observed cosmic microwave background (CMB) temperature map, such as the lack of correlations at large angular separations, remain observationally robust (e.g. [1]). We show that if our universe is flat and has one compact dimension of appropriate size (a.k.a. slab or $R^2 \times S^1$ topology), this would suppress large-angle temperature correlations while maintaining a low- ℓ angular power spectrum consistent with observations. The optimal length appears to be 1.4 times the conformal radius of the CMB’s last scattering surface (χ_{rec}). We construct the probability distribution function of the statistic $S_{1/2}$ using 1000 simulated Sachs-Wolf-only skies for each of several values of L_z/χ_{rec} , while retaining the 3-d Fourier-mode power-spectrum of the best-fit Λ CDM cosmology. For $L_z \simeq 1.4\chi_{\text{rec}}$ the p -value of four standard masked Planck maps is $p \simeq 0.15$, compared to $p \lesssim 0.003$ for the conventional topologically trivial (covering) space. The mean angular power spectrum $\langle C_\ell \rangle$ of the $L_z = 1.4\chi_{\text{rec}}$ slab space matches the observed full-sky power spectrum at $2 \leq \ell \lesssim 6$ – including a substantially suppressed quadrupole C_2 , a slightly suppressed octopole C_3 , and unsuppressed higher multipoles. It does not predict other low- ℓ CMB anomalies, and does not take account of normally sub-dominant Integrated Sachs Wolfe (ISW) contributions. An $L_z = 1.4\chi_{\text{rec}}$ slab topology is consistent with published limits from the Planck maps [3], which require only $L_z \gtrsim 1.12\chi_{\text{rec}}$. It is within the 95% confidence range $1.2 \leq L_z/\chi_{\text{rec}} \leq 2.1$ inferred using the covariance-matrix of temperature fluctuations [4]. However, it violates published circles-in-the-sky limits from WMAP [5] and related unpublished limits from Planck [6], which require $L_z/\chi_{\text{rec}} \gtrsim 1.9$. We remark on the possibility to satisfy these limits, and “postdict” other large-angle anomalies, with closely related topologies.

Cosmic Microwave Background (CMB) data is arguably the best tool extant to determine the topology of the universe. According to General Relativity, the dynamics of spacetime are governed by the Einstein Field Equations, which are local. Global information like topology requires observations, like the CMB, that probe the Universe on the largest scales.

So far, direct searches for spatial topologies using data from WMAP [5] and Planck [3, 7] have found no convincing evidence of compact dimensions below the radius of the last scattering surface (LSS) χ_{rec} – the very nearly spherical locus of points from which most CMB photons we now detect were emitted ~ 13.8 billion years ago.

Meanwhile, analyses of CMB data have revealed a set of anomalous statistical features at large angles that appear incompatible with the null hypothesis that the Universe is statistically homogeneous and isotropic, with primordial fluctuations (generated by inflation) characterizable as Fourier modes with amplitudes that are Gaussian-random statistically independent (GRSI) variables of zero mean [2, 8–15]. One of these anomalies, first

observed by the Cosmic Background Explorer (COBE) satellite [16], concerns the low amplitude of the temperature two-point angular-correlation function (2PACF) on scales above $\sim 60^\circ$, compared with what is expected in the standard inflationary Λ CDM cosmology. Subsequent analyses with both WMAP [2] and Planck [9, 10] data confirmed this anomaly. The reported p -values quantifying the (un)likelihood that this observation is a statistical fluctuation are in the range 0.03% – 0.3%, depending on the details of the analysis performed [9, 10, 17, 18]. A convincing physical explanation appears to require not merely a change in the primordial 3-d power spectrum, but that the amplitudes of Fourier modes are not GRSI.

One way for the Universe to evince statistical anisotropies without altering the local geometry is for it to have non-trivial topology. Topology would enforce boundary conditions on the modes underlying primordial fluctuations – prohibiting some Fourier modes and imposing exact relations among the amplitudes of others. These boundary conditions generically break homogeneity and spherical symmetry, and the resulting primordial fluctuations reflect that symmetry breaking. In the spherical coordinate basis most appropriate for describing CMB observations, correlations will be induced between coefficients $a_{\ell m}$ of spherical harmonics $Y_{\ell m}$, including between those of different ℓ , and consequently between different elements C_ℓ of the angular power spectrum (APS).

*bernui@on.br

†camilapnovaes@gmail.com

‡tspereira@uel.br

§glenn.starkman@case.edu

Correlations between C_{ℓ} s are what is required to realize the observed lack of angular correlations without suppressing the APS over a wide range of ℓ . We show here that a single compact dimension in flat geometry could induce precisely the right correlations. We find that the appropriate size of that dimension, $L_z \simeq 1.4\chi_{\text{rec}}$, is within the 95% confidence range $1.2 \leq L_z/\chi_{\text{rec}} \leq 2.1$ inferred from a Bayesian analysis of the full CMB temperature-temperature correlation function performed using WMAP data [4], and is consistent with published limits obtained using Planck data [3, 7]. However, $L < 2\chi_{\text{rec}}$ implies that the LSS self-intersects, and consequently contradicts published [5] limits $L_z \gtrsim 1.9\chi_{\text{rec}}$ from searches of WMAP full-sky data for the resulting matched circles-in-the-sky (and similar unpublished limits using Planck maps [6]). We discuss below how these strong indications of cosmic topology might be reconciled with the absence of matched circles.

We model our universe by the so-called [19] slab model (T_1 , with topology $R^2 \times S^1$), where one spatial direction is compact while the other two are infinite. The slab is also a phenomenological stand-in [3] for a 3-torus (T_3), where two of the spatial dimensions are large ($L_x, L_y \gg 2\chi_{\text{rec}}$), or for any topology that admits a flat or curved homogeneous geometry in which at certain locations in the fundamental domain the space appears to be compact only in one dimension.

While keeping all of these limits in mind, we nevertheless treat L_z/χ_{rec} as a free parameter and consider specifically $L_z/\chi_{\text{rec}} = \{1.15, 1.4, 1.9\}$. We generate ensembles of realizations of CMB skies for each of these three values of L_z/χ_{rec} and compare to an ensemble of realizations of the covering space $L_z/\chi_{\text{rec}} = \infty$.

Cosmological perturbations can be expanded in a complete basis of eigenfunctions, $Q_{\mathbf{k}}(\mathbf{x})$, of the Laplace operator with the appropriate boundary conditions. In a spatially flat topologically trivial FLRW spacetime, these eigenfunctions can be written as

$$Q_{\mathbf{k}}(\mathbf{x}) = N_k e^{i\mathbf{k}\cdot\mathbf{x}}, \quad \mathbf{k} \in R^3, \quad (1)$$

where N_k is some appropriate normalization. In a slab space $Q_{\mathbf{k}}$ is of the same form, but, taking z to be the compactified direction, k_z assumes only discrete values

$$\mathbf{k} = \left(k_x, k_y, 2\pi \frac{n_z}{L_z} \right), \quad (k_x, k_y) \in R^2, \quad n_z \in Z. \quad (2)$$

As a scalar perturbation, the gravitational potential responsible for the dominant Sachs-Wolfe (SW) contribution to the temperature anisotropies can be expanded as

$$\Phi(\mathbf{x}) = \sum_{\mathbf{k}} \Phi(\mathbf{k}) Q_{\mathbf{k}}(\mathbf{x}), \quad (3)$$

where the sum is over all allowed values of \mathbf{k} . The SW contribution is then written as

$$\Delta T(\hat{\mathbf{x}})_{SW} = \frac{1}{3} \Phi(\mathbf{x} = \chi_{\text{rec}} \hat{\mathbf{x}}), \quad (4)$$

with χ_{rec} being the radius of the CMB sphere in comoving coordinates. Equation (4) neglects the transfer function, which, is nearly constant across the ℓ -range of interest.

Using a Harrison-Zel'dovich approximation to the inflationary power spectrum $P(k)$, we can write $\Phi(\mathbf{k}) = \sqrt{P(k)}\phi(\mathbf{k})$, with $\phi(\mathbf{k})$ a Gaussian random variable of unit variance. Thus

$$\Delta T(\hat{\mathbf{x}})_{SW} = \frac{1}{3} \sum_{\{k\}} \sqrt{P(k)} \sum_{\{\hat{\mathbf{k}}\}_k} e^{ik\chi_{\text{rec}} \cos \theta_{\mathbf{k},\hat{\mathbf{x}}}} \phi(\mathbf{k}), \quad (5)$$

where $\cos \theta_{\mathbf{k},\hat{\mathbf{x}}} = \hat{\mathbf{k}} \cdot \hat{\mathbf{x}}$, and $\phi(\mathbf{k}) = \phi^*(-\mathbf{k})$ enforces Φ 's reality.

For a fixed map resolution, the relation between the multipole ℓ and the wave number \mathbf{k} for SW perturbations is $\ell \sim |\mathbf{k}|\chi_{\text{rec}}$. For large-angle effects, $\ell \leq \ell_{\text{max}} = 20$ suffices. This is less than the $\ell_{\text{max}} = 40$ adopted by the Planck team in their topology-likelihood analyses [3, 7], but is sufficient for our qualitative considerations.

We explore the slab topology with three representative values of L_z/χ_{rec} , namely, model [a] with $L_z/\chi_{\text{rec}} = 1.15$ – just above the published Planck lower limit; model [b] with $L_z/\chi_{\text{rec}} = 1.4$; and [c] with $L_z/\chi_{\text{rec}} = 1.9$ – the published circles-in-the-sky WMAP lower limit. According to Planck, $L_i \geq 2.2\chi_{\text{rec}}$ is indistinguishable from $L_i \rightarrow \infty$, so we take model [d] with $L_z/\chi_{\text{rec}} = 4$ to represent the statistically isotropic covering space.

For each of the four values of L_z/χ_{rec} , we produce 10^3 simulated full-sky SW maps at HEALPix resolution $N_{\text{side}} = 16$ and $2 \leq \ell \leq \ell_{\text{max}} = 20$, i.e., we use (5) to build pixel-space maps then filter out $\ell < 2$ and $\ell > \ell_{\text{max}}$. In building these simulated maps, we should choose

$$n_i \ll \frac{\ell_{\text{max}} L_i}{2\pi \chi_{\text{rec}}}, \quad (6)$$

so we limit n_i to the range $n_i \in (-25, 25)$ in all cases.

For comparison with observations, we have analyzed the four foreground-cleaned CMB maps released by the Planck Collaboration in their second data release [20], namely, the SMICA, NILC, SEVEM, and Commander maps. These are high-resolution maps, with Healpix [21] resolution $N_{\text{side}} = 2048$. We extracted the multipoles $2 \leq \ell \leq 20$, and rebuilt these maps using $N_{\text{side}} = 16$.

The Planck team also released a variety of masks [20] associated with each of the four full-sky maps. The UT78 mask is the union of the confidence masks associated with each map; it includes a fraction $f_{\text{sky}} = 0.78$ of the sky. This mask was also downgraded to $N_{\text{side}} = 16$, masking a pixel in the downgraded map if at least 50% of the underlying high-resolution pixels are masked. The resulting UT80 mask, used in all our analyses, has $f_{\text{sky}} = 0.80$.

Because the slab topology breaks statistical isotropy, the orientation of the slab with respect to the Galaxy (i.e. mask) matters. For $L_z/\chi_{\text{rec}} = 1.15, 1.4$, and 1.9 we therefore consider four illustrative cases with the slab's normal vector pointing in the directions (in galactic coordinates): [i] $(l, b) = (0^\circ, 90^\circ)$ the north galactic pole

(NGP); [ii] $(l, b) = (240^\circ, -20^\circ)$; [iii] $(l, b) = (270^\circ, 0^\circ)$; [iv] $(l, b) = (240^\circ, 70^\circ)$.

Following [22], we renormalized each set of 10^3 slab simulations by a factor that matched their mean APS in the range $15 \leq \ell \leq 20$ to that from the Planck maps. The renormalized APS of the three simulated slab-topology data sets, for direction [i], and the statistically isotropic data set are plotted in figure 1, along with the Planck APS for comparison. The grey and blue bands are the cosmic-variance bands for, respectively, the statistically isotropic model and $L_z/\chi_{\text{rec}} = 1.4$. (Note, however, that the C_ℓ are not statistically independent in the slab topology.)

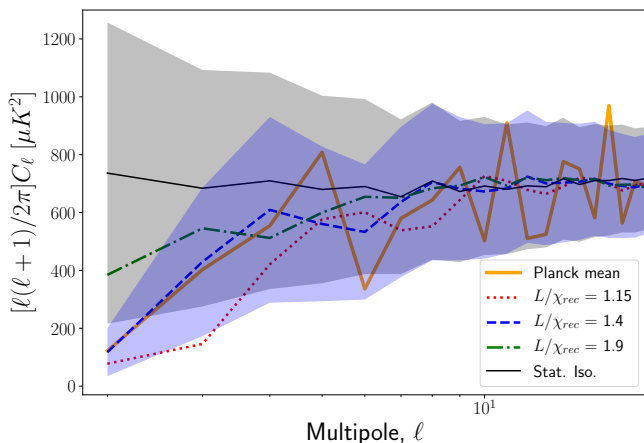


FIG. 1: Mean angular power spectrum of the data sets in the slab topology model with $L_z/\chi_{\text{rec}} = \{1.15, 1.4, 1.9\}$ (with orientation [i]), and in the statistically isotropic (SI) Λ CDM model. The “Planck mean” curve is the arithmetic mean of the spectra from the four foreground-cleaned Planck maps. The shaded areas correspond to “one-sigma” cosmic-variance bands around the SI (grey) and $L_z/\chi_{\text{rec}} = 1.4$ (blue) models.

We wish to quantify the angular correlations from our simulations, and compare them with one another and observations. The standard estimator of angular correlations in a map is the two-point angular correlation function (2PACF) [12, 16, 23]

$$C(\theta) \equiv \frac{1}{N_p} \sum_{i,j} \Delta T(\hat{\mathbf{x}}_i) \Delta T(\hat{\mathbf{x}}_j) |_{\hat{\mathbf{x}}_i \cdot \hat{\mathbf{x}}_j = \cos \theta}, \quad (7)$$

the sum running over all pairs of pixels separated by $\theta = \arccos(\hat{\mathbf{x}}_i \cdot \hat{\mathbf{x}}_j)$. Because the monopole and dipole of the CMB are large compared to higher multipoles, and predominantly of different origins, we redefine $C(\theta) \rightarrow C(\theta) - \frac{1}{4\pi} (C_0 + 3C_1 \cos \theta)$. As is conventional, if confusing, we refer below to this modified 2PACF as the 2PACF, and write simply $C(\theta)$.

We calculate $C(\theta)$ for all the simulated maps with the UT80 mask, obtaining thirteen ensembles each of 10^3 functions $\{C(\theta)\}$, corresponding to the four values of L_z/χ_{rec} and (for $L_z/\chi_{\text{rec}} = 1.15, 1.4, 1.9$) the four orientations. For each of these, we compute the correspond-

ing mean cut-sky 2PACF, $\overline{C}(\theta)$. We plot them in figure 2 for orientation [i]. (The other orientations prove nearly indistinguishable.) We also plot the mean 2PACF of the four Planck maps. To give the reader a sense of the uncertainties, we include the “one-sigma” error bands for the statistically isotropic case (grey) and for the $L_z/\chi_{\text{rec}} = 1.4$ slab (blue); however, we caution that $C(\theta)$ for different values of θ are correlated.

We see in figure 2 that the observed 2PACF at large angles ($\theta \gtrsim 60^\circ$) is much closer to zero than one would expect from the statistically isotropic case. This is the well-known “large-angle” angular-correlation anomaly.

Figures 1 and 2 clearly show that the CMB angular correlations are sensitive to the size of the slab in the way one might expect: smaller slabs yield lower values of C_ℓ at very low- ℓ and result in suppressed $C(\theta)$ at large θ . More specifically, large-angle correlations can exhibit noticeable suppression over a broad range of angular separations θ without strongly suppressing the APS over a broad range of ℓ . Much like the data.

We call the reader’s particular attention to the blue-dashed curves for $L_z/\chi_{\text{rec}} = 1.4$ in figures 1 and 2 and their similarity to the curves for the Planck mean (solid orange), and contrasted to the statistically isotropic simulations (solid black).

The very-low- ℓ APS for $L_z/\chi_{\text{rec}} = 1.4$ exhibits the same pattern as does the Planck mean – marked quadrupole (C_2) suppression (relative to the SI), mild octopole (C_3) suppression, and no noticeable suppression of C_ℓ for higher ℓ . The $L_z/\chi_{\text{rec}} = 1.4$ simulations do not reproduce the observed pattern of odd- ℓ C_ℓ being larger than even- ℓ ones known as the parity anomaly. This is unsurprising since the slab topology has a preferred axis ($\pm \hat{z}$ – the normal to the slab faces) but no preferred direction. See below for further discussions.

The 2PACF for $L_z/\chi_{\text{rec}} = 1.4$ also exhibits remarkably close to the same pattern as does the Planck mean – the same zero crossing at $\theta \simeq 30^\circ$, the same approximately zero value above $\theta \simeq 75^\circ$. Qualitatively, it lacks only the anti-correlation for $\theta \gtrsim 160^\circ$, which could be connected to residual Galaxy contamination [18].

To characterize how (im)probable is the observed lack of large-angle CMB temperature correlations in the context of any particular model, we use the well-known statistic

$$S_{1/2} \equiv \int_{-1}^{1/2} [C(\theta)]^2 d(\cos \theta). \quad (8)$$

$S_{1/2}$ was first proposed by the WMAP team [2] and has since been used extensively (see [12] for a review).

We compute $S_{1/2}$ for each of the simulated maps and the four foreground-cleaned Planck maps [10] and construct a probability density function (PDF) for each value of L_z/χ_{rec} and each slab orientation. The p -values of the $S_{1/2}$ statistic for each topology with slab orientation [i], relative to each of the four Planck maps, is listed in Table I. In Table II we show the p -values of the four

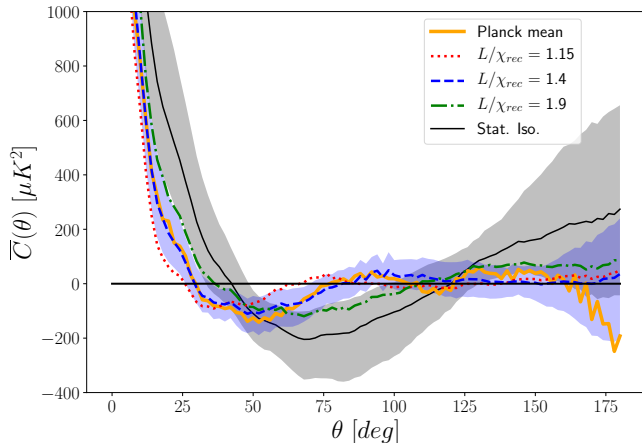


FIG. 2: Mean 2PACF $\overline{C}(\theta)$ from simulations of a slab topology with $L_z/\chi_{\text{rec}} = \{1.15, 1.4, 1.9\}$ (with orientation [i]), and from the statistically isotropic Λ CDM simulations. “One-sigma” cosmic-variance regions for $L_z/\chi_{\text{rec}} = 1.4$ (blue) and SI (grey) are shown.

CMB maps	$\log[S_{1/2}]$	p (%) [a]	p (%) [b]	p (%) [c]	p (%) [d]
SMICA	3.39	40.0	15.2	3.3	0.3
SEVEM	3.40	41.9	15.7	3.6	0.3
NILC	3.42	43.9	17.0	3.8	0.3
Commander	3.43	45.1	17.5	4.1	0.4

TABLE I: p -values for the PDF of the $S_{1/2}$ values obtained comparing the four foreground-cleaned Planck maps [20] to ensembles of 10^3 simulations for each of the $L_z/\chi_{\text{rec}} = (1.15, 1.4, 1.9, \infty)$ (respectively models [a], [b], [c] and [d].)

topologies in comparison with $S_{1/2}^{\text{SMICA}}$, for the four chosen directions ([i]-[iv]).

For the simply connected (statistically isotropic) case [d], these p -values are consistent with those found in [10] and quite small, $p \simeq 0.3\%$. Smaller L_z increases that p .

The smallest slab ($L_z = 1.15\chi_{\text{rec}}$) produces quite high p -values ($p \simeq 40\%$) but appears, at least by eye to over-suppress large-angle $C(\theta)$ and low- ℓ C_ℓ . The largest slab ($L_z = 1.9\chi_{\text{rec}}$) produces significant gains in the $S_{1/2}$ p -value compared to the covering space ($p \simeq 3\%$), but seems to under-suppress $C(\theta)$ and low- ℓ C_ℓ . $L_z = 1.4\chi_{\text{rec}}$ appears to be the Goldilocks value – just the right suppression of both $C(\theta)$ and C_ℓ , and a credible $p \simeq 15\%$ for the observed $S_{1/2}$. We caution the reader that a simple chi-square test is inconclusive in deciding among the models for $C(\theta)$.

A Bayesian analysis carried out by the Planck team with their 2015 data found that, for the slab topology, $L > 1.12\chi_{\text{rec}}$ at the 99% confidence level [3]. Despite including a back-to-back matched-circles search [24] applicable to the slab topology, this Planck limit is unexpectedly weaker than the equivalent WMAP limit of $L_z \gtrsim 1.9\chi_{\text{rec}}$ [5]. However, the Planck circle search, used

Orientation \ data sets	p (%) [a]	p (%) [b]	p (%) [c]	p (%) [d]
[i]	40.4	15.2	3.3	0.3
[ii]	43.2	14.3	4.3	0.3
[iii]	39.1	12.2	3.5	0.3
[iv]	36.4	10.8	3.1	0.3

TABLE II: p -values for $S_{1/2}$ of the SMICA map among simulated ensembles for $L_z/\chi_{\text{rec}} = (1.15, 1.4, 1.9, \infty)$ (i.e., models [a], [b], [c] and [d]); and for the four orientations specified in the text.

a sky with approximately 25% of the pixels masked – mostly near the Galactic plane. Such masking is typically dictated by the presence of Galactic foregrounds. The matched circles (or other correlations) of a slab topology are easily hidden in the masked region. In contrast, the WMAP search recognized that the circle search relies predominantly on the Sachs-Wolfe effect at the LSS, which is dominated by contributions in the first Doppler peak of the CMB at $\ell \simeq 200$. This small-angular-scale signal is believed to be accurately represented in full-sky foreground-cleaned maps, so [5] used the full-sky Independent Linear Combinations (ILC) map, originally developed precisely for this search. The same search was repeated for the Planck 2013 maps, and a marginally more stringent unpublished limit was obtained [6]. A $L_z/\chi_{\text{rec}} = 1.4$ slab topology is thus firmly ruled out.

Meanwhile, the slab topology also does not explain other large-angle anomalies – the parity anomaly [25], the dipole asymmetry [13] (a.k.a. low northern variance [15, 26]), quadrupole-octopole planarity and alignment [27].

Conclusions: Large-angle CMB anomalies discovered in COBE or WMAP data persist after Planck. No satisfactory explanation has yet been proposed. We have explored the lack of large-angle correlations as a possible manifestation of a compact direction in the Universe, as modeled by the slab topology $R^2 \times S^1$. We considered ensembles of simulated CMB maps consistent with a single compact dimension of size $L_z/\chi_{\text{rec}} = 1.15, 1.4, 1.9$ relative to the LSS. We compared their ability to reproduce Planck observations with simulations of the flat covering space.

In a slab topology, the Sachs-Wolfe temperature fluctuations were able to reproduce the observed suppression of large-angle correlations (small $C(\theta \gtrsim 60^\circ)$ leading to small $S_{1/2}$) simultaneously with the observed low- ℓ angular power spectrum, with its heavily suppressed quadrupole, mildly suppressed octopole, and unsuppressed higher multipoles (relative to the covering space). A slab space with $L_z/\chi_{\text{rec}} = 1.4$ best reproduced the qualitative features of $C(\theta)$ and C_ℓ seen in Planck maps, and increased the p -value of $S_{1/2}$ from the covering space’s $\sim 0.3\%$ to $\sim 15\%$. The ISW will not spoil low $S_{1/2}$ [28].

Yet, a $L_z = 1.4\chi_{\text{rec}}$ compact dimension is in conflict with limits from WMAP and Planck. Also, this topol-

ogy would not explain other statistically significant large-angle anomalies. This suggests that if topology is indeed the explanation of the lack of large angle correlations, the vanilla slab may not be the full story.

There are simple variations on the slab topology in flat geometry that might build on the slab's success and mitigate its failures. Wider exploration would allow for rotations (about the slab normal) or transverse rotations, either of which could relieve the matched-circles constraint; they might also incorporate identifications in the dimensions transverse to the slab normal to help explain other anomalies. There are also topologies of curved space that for large curvature radius can look like a slab for a well-placed observer [29]. These may be intriguing, given the preference for small positive curvature ($\Omega_k \simeq 0.04 \pm 0.03$) in high-redshift Planck data (TT+TE+EE+lowE) [30].

The agreement between the slab topology and observations at the largest angles and lowest ℓ is highly sug-

gestive. We may be seeing the first evidence that the Universe is not infinite, or at least not infinite in all directions. A more intensive search for cosmic topology is merited.

We acknowledge a PVE project from CAPES (Science without Borders program 88881.064966/2014-01). CPN and AB acknowledge fellowships from the Brazilian Agencies FAPERJ and CNPq, respectively. TSP thanks the Conselho Nacional de Desenvolvimento Científico e Tecnológico (grant #311732/2015-1) and Fundação Araucária (PBA 2016) for their support. GDS is supported by Department of Energy grant DE-SC0009946 to CWRU, and thanks the Observatório Nacional for its hospitality. This paper made use of observations obtained with Planck, an ESA science mission funded by ESA Member States, NASA, and Canada. Some of the results in this paper have been derived using the HEALPix/healpy package [21].

-
- [1] D. J. Schwarz, C. J. Copi, D. Huterer and G. D. Starkman, *Class. Quant. Grav.* **33**, no. 18, 184001 (2016).
- [2] D. N. Spergel, *et al.*, *Astrophys. J. Suppl.* **148**, 175 (2003).
- [3] P. A. R. Ade *et al.* [Planck Collaboration], *Astron. Astrophys.* **594**, A18 (2016).
- [4] G. Aslanyan, A. V. Manohar, *JCAP* **06**, id. 003 (2012).
- [5] N. J. Cornish, D. N. Spergel, G. D. Starkman and E. Komatsu, *Phys. Rev. Lett.* **92**, 201302 (2004); J. S. Key, N. J. Cornish, D. N. Spergel and G. D. Starkman, *Phys. Rev. D* **75**, 084034 (2007); P. Bielewicz, A. J. Banday, *M.N.R.A.S.* **412**, 2104 (2011); P. M. Vaudrevange, G. D. Starkman, N. J. Cornish and D. N. Spergel, *Phys. Rev. D* **86**, 083526 (2012); R. Aurich, S. Lustig, *M.N.R.A.S.* **433**, 2517 (2013).
- [6] P. M. Vaudrevange, G. D. Starkman, N. J. Cornish and D. N. Spergel (unpublished)
- [7] P. A. R. Ade *et al.* [Planck Collaboration], *Astron. Astrophys.* **571**, A26 (2014).
- [8] C. L. Bennett, *et al.*, *Astrophys. J. Suppl.* **192**, 17 (2011).
- [9] P. A. R. Ade, *et al.*, *Astron. Astrophys.* **571**, A23 (2014);
- [10] P. A. R. Ade *et al.* [Planck Collaboration], *Astron. Astrophys.* **594**, A16 (2016).
- [11] C. J. Copi, D. Huterer, G. D. Starkman, *Phys. Rev. D* **70**, 043515 (2004).
- [12] C. J. Copi, D. Huterer, D. J. Schwarz, G. D. Starkman, *Adv. Astron.* **2010**, 78 (2010).
- [13] H. K. Eriksen, F. K. Hansen, A. J. Banday, K. M. Górski, P. B. Lilje, *Astrophys. J.* **605**, 14 (2004);
- [14] F. K. Hansen, A. J., Banday, K. M. Górski, *M.N.R.A.S.* **354**, 641 (2004); A. Bernui, *Phys. Rev. D* **80**, 123010 (2009); A. Gruppuso, P. Natoli, F. Paci, F. Finelli, D. Molinari, A. De Rosa, N. Mandolesi, *JCAP* **07**, 047 (2013); A. Bernui, A. F. Oliveira, T. S. Pereira, *JCAP* **10**, 041 (2014); L. Polastri, A. Gruppuso, P. Natoli, *JCAP* **1504**, 018 (2015).
- [15] Y. Akrami *et al.*, *Astrophys. J.* **784**, L42 (2014);
- [16] G. Hinshaw *et al.*, *Astrophys. J. Lett.* **464**, L25 (1996).
- [17] C. J. Copi, D. Huterer, D. J. Schwarz, G. D. Starkman, *M.N.R.A.S.* **367**, 79 (2006); *Phys. Rev. D* **75**, 023507 (2007); *M.N.R.A.S.* **399**, 295 (2009); *M.N.R.A.S.* **451**, 2978 (2013); A. Hajian, arXiv:astro-ph/0702723 (2007); G. Efstathiou, Y.-Z. Ma, D. Hanson, *M.N.R.A.S.* **407**, 2530 (2010); J. Kim, P. Naselsky, *Phys. Rev. D* **82**, 063002 (2010); *Astrophys. J.* **739**, id. 79 (2011); A. Gruppuso, *M.N.R.A.S.* **437**, 2076 (2014).
- [18] C. J. Copi, D. Huterer, D.J. Schwarz, G. D. Starkman, *M.N.R.A.S.* **399**, 295 (2009).
- [19] C. Adams and J. Shapiro, *American Scientist* **89**, 443 (2001).
- [20] R. Adam *et al.* [Planck Collaboration], *Astron. Astrophys.* **594**, A9 (2016)
- [21] Górski, K.M., Hivon, E. & Wandelt, B.D. astro-ph/9812350 and <http://www.eso.org/science/healpix/> (1998).
- [22] R. Aurich, H. S. Janzer, S. Lustig, F. Steiner, *Class. Quantum Grav.* **25**, 125006 (2008).
- [23] A. Bernui, A. F. F. Teixeira, astro-ph/9904180 (1999).
- [24] N. J. Cornish, D. N. Spergel and G. D. Starkman, gr-qc/9602039 (1996); N. J. Cornish, D. N. Spergel and G. D. Starkman, *Proc. Nat. Acad. Sci.* **95**, 82 (1998); N. J. Cornish, D. Spergel and G. Starkman, *Phys. Rev. D* **57**, 5982 (1998); N. J. Cornish, D. N. Spergel and G. D. Starkman, *Class. Quant. Grav.* **15**, 2657 (1998).
- [25] J. Kim and P. Naselsky, *Astrophys. J.* **714**, L265 (2010)
- [26] M. O'Dwyer, C. J. Copi, L. Knox and G. D. Starkman, *Mon. Not. Roy. Astron. Soc.* **470**, no. 1, 372 (2017)
- [27] A. de Oliveira-Costa, M. Tegmark, M. Zaldarriaga and A. Hamilton, *Phys. Rev. D* **69**, 063516 (2004)
- [28] C. J. Copi, M. O'Dwyer and G. D. Starkman, *Mon. Not. Roy. Astron. Soc.* **463**, no. 3, 3305 (2016)
- [29] J. Weeks, R. Lehoucq and J. P. Uzan, *Class. Quant. Grav.* **20**, 1529 (2003).
- [30] N. Aghanim *et al.* [Planck Collaboration], arXiv:1807.06209 [astro-ph.CO].